Journal of Power Sources 226 (2013) 219–222

Contents lists available at SciVerse ScienceDirect

Journal of Power Sources

journal homepage: www.elsevier.com/locate/jpowsour

Short communication

# Electrochemical performance of $LiCo_{1/3}Mn_{1/3}Ni_{1/3}O_2$ hollow spheres as cathode material for lithium ion batteries

Chaofan Yang, Junjie Huang*, Liangai Huang, Gaojun Wang

*College of Chemistry and Chemical Engineering, Shaoxing University, Shaoxing 312000, PR China*

## HIGHLIGHTS

- $LiCo_{1/3}Mn_{1/3}Ni_{1/3}O_2$ hollow spheres are prepared firstly by a template method.
- $LiCo_{1/3}Mn_{1/3}Ni_{1/3}O_2$ hollow spheres are constructed by many nanoparticles.
- Many pores on the wall of spheres benefit for wetting particles by electrolyte.
- This material presents a super rate capability (10C: 91.5 mAh $g^{-1}$).

## ARTICLE INFO

*Article history:*
Received 14 August 2012
Received in revised form
30 October 2012
Accepted 31 October 2012
Available online 8 November 2012

*Keywords:*
$LiCo_{1/3}Mn_{1/3}Ni_{1/3}O_2$
Hollow sphere
Cathode material
Template

## ABSTRACT

$LiCo_{1/3}Mn_{1/3}Ni_{1/3}O_2$ hollow spheres with an average outer diameter of 300 nm and a wall thickness of about 50 nm are prepared by using carbon spheres as template. They demonstrate excellent electrochemical performance, including high discharge capacity and rate capability. At a current rate of 0.2C (34 mA $g^{-1}$, 0.34 mA $cm^{-2}$), cathode materials constituted by the hollow spheres display a discharge capacity of 175.4 mAh $g^{-1}$. Even at a current rate of 10C (1700 mA $g^{-1}$, 17 mA $cm^{-2}$), the discharge capacity also keeps at 91.5 mAh $g^{-1}$. The reasons lie in that the hollow structure has a large surface to contact with liquid electrolyte, resulting in a better electrochemical performance at high charge/discharge rate.



## 1. Introduction

$LiCo_{1/3}Mn_{1/3}Ni_{1/3}O_2$, a promising cathode material, has attracted much attention as a possible replacement for $LiCoO_2$ due to its multiple advantages, such as a high theoretical capacity, almost zero phase change when charged/discharged in the voltage range of 2.5–4.4 V, good thermal stability, low cost and low toxicity [1–3]. Its electrochemical performance is influenced greatly by crystal structure, grain size, surface area and porosity [4–6]. To explore the capability of $LiCo_{1/3}Mn_{1/3}Ni_{1/3}O_2$, different procedures were developed to obtain high quality $LiCo_{1/3}Mn_{1/3}Ni_{1/3}O_2$ materials, such as solid state method [7], sol-gel method [8], coprecipitation method [9,10] and molten salt method [11]. Compared with micrometer grains, nano particles have larger surface area for lithium insertion and shorter pathway for lithium diffusion. Recently, $LiCo_{1/3}Mn_{1/3}Ni_{1/3}O_2$ with Nano structures have been prepared [12,13], which showed an improved performance when used as cathode material. However, in most commercial battery systems, the separator has pores, so if the nano particles are released from the electrode surface, they may penetrate the separator and reach the other electrode, resulting in a capacity loss. To avoid the shortcomings of nano particles, an alternative approach is designed to prepare porous micrometer material constructed by nano primary particles [14–16], thus maintaining good particle–particle contact and adequate particle size, while maximizing the rate capability. Sinha et al., obtained a porous $LiCo_{1/3}Mn_{1/3}Ni_{1/3}O_2$ material through polymer template route, which presented a relatively high rate capability [17].

Mono-dispersed hollow spherical materials have attracted more and more attentions in high power batteries due to their characteristic features, such as large surface areas and open pores [18–21]. The present work aims to improve the charge/discharge performance at high rates by using $LiCo_{1/3}Mn_{1/3}Ni_{1/3}O_2$ hollow spheres as a cathode material. These hollow spheres are fabricated with carbon sphere templates, which were prepared through a hydrothermal route with glucose as a raw material. Carbon spheres have

* Corresponding author. Tel.: +86 575 88342606; fax: +86 575 88341528.
*E-mail address:* hjj@zscas.edu.cn (J. Huang).

0378-7753/$ – see front matter © 2012 Elsevier B.V. All rights reserved.
http://dx.doi.org/10.1016/j.jpowsour.2012.10.089

many −COOH and −OH groups on their surfaces, which have strong abilities to absorb metallic ions, thus carbon spheres were often used as template for the preparation of hollow metallic oxides' spheres [22–24]. Among the introduced methods of $LiCo_{1/3}Mn_{1/3}Ni_{1/3}O_2$ preparation, the coprecipitation way is used widely, but in order to get a multicomponent solid solution, experimental conditions such as pH value, temperature and speed of mixing must be carefully controlled due to the different solubility product of the hydroxide or carbonate of $Co^{2+}$, $Mn^{2+}$ and $Ni^{2+}$. Unlike the coprecipitation method, the carbon sphere template method allows the surface −COOH and −OH groups to adsorb non-selectively the ions of $Li^+$, $Co^{2+}$, $Mn^{2+}$ and $Ni^{2+}$, resulting in a mixture of these ions on the surface of carbon spheres at atomic level, and forming a multicomponent solid solution. Furthermore, in the calcination process, carbon sphere template not only has the function to form a cavity, but also can effectively avoid the particles' aggregation. In the present study, the fabrication and electrochemical performance of hollow $LiCo_{1/3}Mn_{1/3}Ni_{1/3}O_2$ spheres are investigated.

## 2. Experimental section

Preparation of carbon template spheres: In a typical procedure, glucose (6 g, analytic purity, Beijing Chemical Reagent Factory) was dissolved in distilled water (35 ml) to form a clear solution. This solution was then sealed in a 40 ml teflon-lined autoclave and maintained at 180 °C for 10 h. The black or puce products were centrifuged at 5000 rpm for 20 min. The products were redispersed, washed and centrifuged in water, and this cycle was repeated five times. Next, the products were isolated after being centrifuged, washed, and redispersed in alcohol, and this cycle was repeated five times. The spheres were then oven-dried at 80 °C for 10 h.

Preparation of $LiCo_{1/3}Mn_{1/3}Ni_{1/3}O_2$ hollow spheres: a solution was first obtained by dissolving 2 mmol $Co(CH_3COO)_2$, 2 mmol $Mn(CH_3COO)_2$, 6.6 mmol $LiCH_3COO$ and 2 mmol $Ni(NO_3)_2$ in a mixed solvent (0.5 ml distilled water + 1.5 ml ethanol), then carbon spheres (200 mg) were added, and a suspension solution was obtained. The solvent was evaporated slowly under a constant ultrasonic means at 80 °C until a dried powder was obtained, then calcinated at 800 °C for 5 h with a temperature ramp of 1 °C/min from room temperature to 800 °C in the air. After cooling down, the $LiCo_{1/3}Mn_{1/3}Ni_{1/3}O_2$ hollow spheres were obtained. All the reagents used are available from Sinopharm Company.

X-ray diffraction (XRD) patterns were recorded on a Bruker D8 advanced diffractometer with Cu Kα radiation. The morphology of $LiCo_{1/3}Mn_{1/3}Ni_{1/3}O_2$ hollow spheres was characterized by both scanning electron microscopy (SEM) (JEOL JSM-6360LV) and transmission electron microscope (TEM) (JEOL JEM-1011).

Electrochemical measurements were performed using a 2016 coin-cell composed of a $LiCo_{1/3}Mn_{1/3}Ni_{1/3}O_2$ cathode and a lithium metal anode separated by a microporous polyethylene film. The cathode was prepared by mixing the active material with conductive carbon black and PTFE in a weight ratio of 80:15:5. The mixture was firstly spread onto an aluminum foil (20 μm thickness), and proceeded with a rolling press, finally dried under vacuum at 363 K for 10 h. The active material loading amount of the electrodes is about 10 mg/cm$^2$ for all the electrochemical tests and the thickness of the active material layer is about 25 μm. The coin-cell was assembled in an argon-filled glove box, and the electrolyte is 1 mol L$^{-1}$ $LiPF_6$-EC/DMC (1:1, v/v). The charge–discharge cycling test was carried out galvanostatically at different current densities on Electrochemical Analyzer (Wuhan Land Electrochemical Equipment Company, China). The cut-off voltages for charge and discharge processes are 4.4 and 2.5 V, respectively. The impedance spectra (10 mHz to 100 kHz, 5 mV perturbation) were recorded at EG&G 5210 lock-in amplifier and 273A potentiostat/galvanostat. Experiments were carried out at room temperature.

## 3. Results and discussion

Fig. 1A shows the SEM image of carbon templates. It can be clearly observed that the carbon spheres had a narrow size distribution with an average diameter of about 2.0 μm and connected to each other, forming a net structure. Fig. 1B and C shows the SEM and TEM morphology of the obtained $LiCo_{1/3}Mn_{1/3}Ni_{1/3}O_2$ powder, respectively. Many hollow spheres with a diameter of about 300 nm can be observed clearly. From the TEM image (the inner picture), these hollow spheres have a wall thickness of about 50 nm and are constructed by many $LiCo_{1/3}Mn_{1/3}Ni_{1/3}O_2$ nanoparticles. Two types of pores can be found, large pores and small pores as shown in Fig. 1C. Large pores are constructed by the $LiCo_{1/3}Mn_{1/3}Ni_{1/3}O_2$ hollow spheres, which diameters are higher than 100 nm. Small pores are located on the wall of the $LiCo_{1/3}Mn_{1/3}Ni_{1/3}O_2$ hollow spheres, which diameters are lower than 100 nm. Small pores are created by the overflow of gas originated from the decomposition or oxidation of carbon spheres during the calcination process. Compared with the diameter of carbon templates, the $LiCo_{1/3}Mn_{1/3}Ni_{1/3}O_2$ hollow spheres have a large shrinkage, which were also found in the preparation of $Ga_2O_3$ and GaN hollow spheres using carbon spheres as template [22]. The possible explanation should be the further dehydration of the loosely cross-linked structure of the carbon spheres in the calcination process, which leads to the densification of $LiCo_{1/3}Mn_{1/3}Ni_{1/3}O_2$ precursors in the surface layer of template, resulting in a smaller diameter. The formation mechanism of $LiCo_{1/3}Mn_{1/3}Ni_{1/3}O_2$ hollow spheres is as follows: as shown in literature [24], there are many $-COO^-$ and −

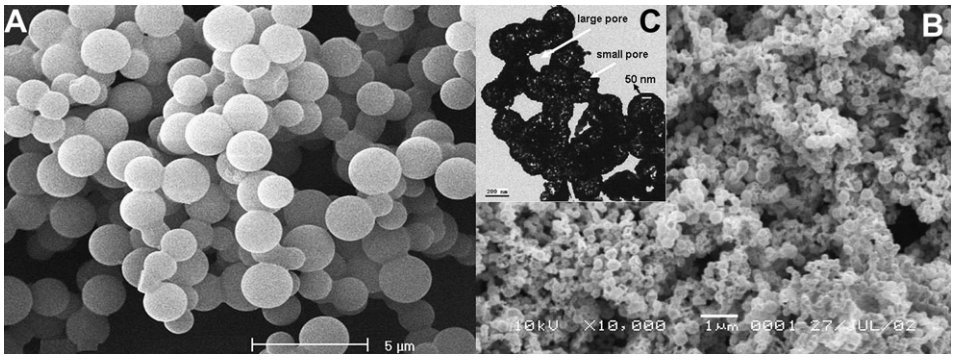


**Fig. 1.** SEM images of (A) carbon spheres, (B) $LiCo_{1/3}Mn_{1/3}Ni_{1/3}O_2$ hollow spheres and TEM image of (C) $LiCo_{1/3}Mn_{1/3}Ni_{1/3}O_2$ hollow spheres.

OH groups on the surface of carbon spheres, which have strong bonding ability with metal ions, therefore, in the suspension solution, $Li^+$, $Co^{2+}$, $Mn^{2+}$and $Ni^{2+}$ can be adsorbed on the surface of carbon spheres. Calcinated in the air, the carbon spheres were oxidized to CO or $CO_2$, leaving cavities.

Fig. 2 shows the XRD pattern of $LiCo_{1/3}Mn_{1/3}Ni_{1/3}O_2$ hollow spheres, in which all peaks are indexed as the hexagonal a-$NaFeO_2$ structure with a space group of R-3m [1]. No obvious impurity peaks are found. The peaks (assigned to the Miller indices (101), (006) and (102); (108) and (110), respectively) have a good splitting, indicating the obtained $LiCo_{1/3}Mn_{1/3}Ni_{1/3}O_2$ materials have a super layered structure [4,25]. The integrated intensity ratio of (003)/(104) is 1.86, which is larger than 1.2, indicating low cation mixing and a homogeneous distribution of cations within the structure. The lattice parameters *a*, *c* and *c*/*a* were given as 2.859, 14.237 Å and 4.980, respectively, which is similar to the values reported previously [14,15]. The high *c*/*a* value also indicates small cation mixing and good ordering of the transition metal ions in the metal layer.

The charge–discharge curves of $LiCo_{1/3}Mn_{1/3}Ni_{1/3}O_2$ electrode at different current rates from 0.2 (34 mA $g^{-1}$, 0.34 mA $cm^{-2}$) to 10C (1700 mA $g^{-1}$, 17 mA $cm^{-2}$) are shown in Fig. 3. In each rate, the charge/discharge process was taken by 10 cycles, and the curves in Fig. 3 were recorded in the second cycle at each rate. In each curve of the rates lower than 10C, a plateau at around 3.6–3.8 V can be observed clearly during the discharge processes, which matches well with the typical layer-structured $LiCo_{1/3}Mn_{1/3}Ni_{1/3}O_2$ reported by other groups [26,27]. Even discharged at 10C, the charge/discharge curves are also very smooth, suggesting the electrode structures are stable and provide a favorable network for fast lithium kinetics [16]. At the rate of 0.2C, the cathode discharge capacity is 175.4 mAh $g^{-1}$, which is higher than the values reported in the literatures at similar rates, for example, 163.5 mAh $g^{-1}$ at 0.1C (nanoparticles) [13], 173.9 mAh $g^{-1}$ at 0.1C (porous structured $LiCo_{1/3}Mn_{1/3}Ni_{1/3}O_2$) [4]. When the rate is increased to 0.5, 1, 2, 5 and 10C, the discharge capacity keeps at the value of 168, 158, 145, 122 and 91.5 mAh $g^{-1}$ respectively. This excellent rate capability is mainly due to the hollow structure, which allows the electrolyte to penetrate easily into every $LiCo_{1/3}Mn_{1/3}Ni_{1/3}O_2$ particles, making the insertion/extraction of $Li^+$ easy between liquid electrolyte and $LiCo_{1/3}Mn_{1/3}Ni_{1/3}O_2$ particles. Furthermore, hollow structured materials have more contacts between $LiCo_{1/3}Mn_{1/3}Ni_{1/3}O_2$ particles and conductive carbon in comparison with densely packed $LiCo_{1/3}Mn_{1/3}Ni_{1/3}O_2$ grains [28], hence, improving the electronic conductivity. This may also help to improve the high rate performance. In addition, the hollow spheres are constructed by many

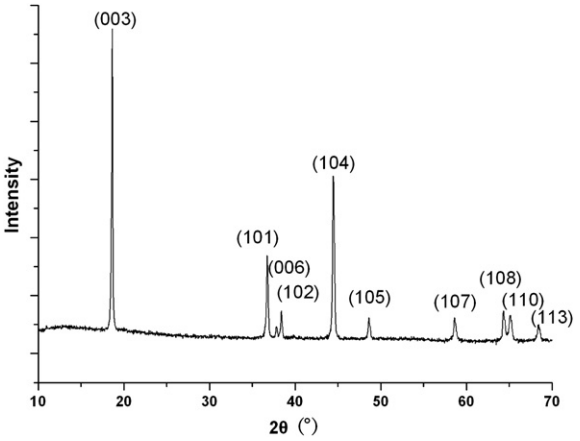


**Fig. 2.** XRD pattern of $LiCo_{1/3}Mn_{1/3}Ni_{1/3}O_2$ hollow spheres.

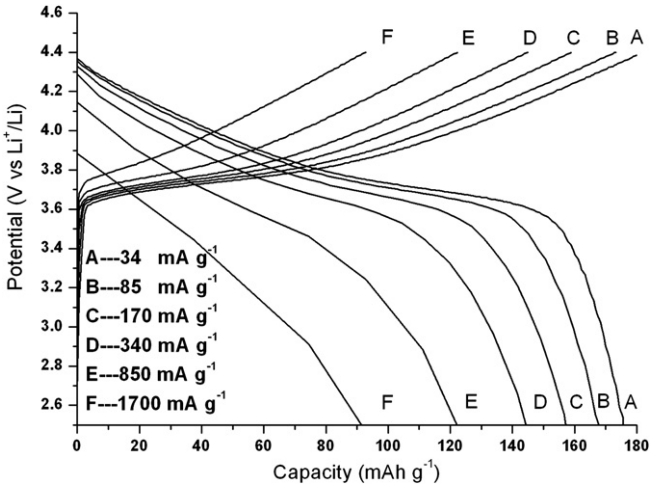


**Fig. 3.** Charge and discharge curves of $LiCo_{1/3}Mn_{1/3}Ni_{1/3}O_2$ electrode at different current rates.

$LiCo_{1/3}Mn_{1/3}Ni_{1/3}O_2$ nanoparticles, which facilitate the fast transfer of electrons and allow a short pathway for fast lithium diffusion in $LiCo_{1/3}Mn_{1/3}Ni_{1/3}O_2$ particles.

The electrochemical impedance spectra (EIS) of the Li/$LiCo_{1/3}Mn_{1/3}Ni_{1/3}O_2$ cell are given in Fig. 4. Curves A and B were recorded at a potential of 2.83 V before the first charge/discharge cycle and at a potential of 3.75 V in the third charging process, respectively. Each curve consists of a semicircle in the high frequency region and one straight line with near 45° slope in the low frequency region, which is similar to the results of porous $LiCo_{1/3}Mn_{1/3}Ni_{1/3}O_2$ materials reported in literature [4,15]. The semicircle of the Cole–Cole plot was ascribed to the charge transfer through the surface layer of $LiCo_{1/3}Mn_{1/3}Ni_{1/3}O_2$ particles [15]. The straight line in the low frequency region corresponds to the semi-infinite diffusion process of $Li^+$. The cell has a smaller diameter of semicircle in the third charging process in comparison with that before the first charge/discharge cycle, indicating a decrease of resistance to charge transfer due to activation in the first cycle [29]. The small charge transfer resistance indicates a fast lithium ion migration through the interface between the surface layer of the particles and the electrolyte.

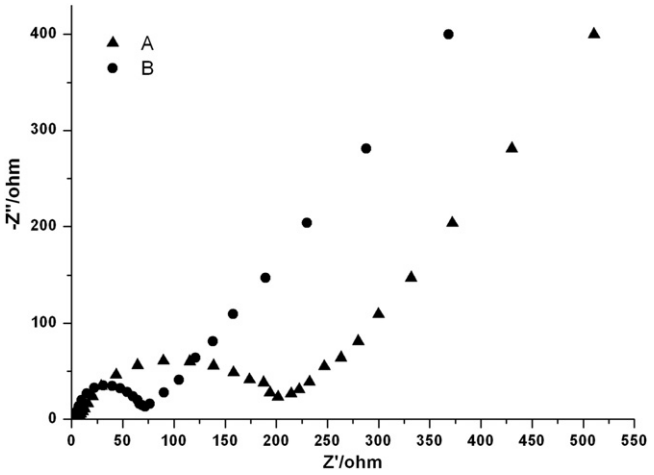


**Fig. 4.** Impedance spectra of $LiCo_{1/3}Mn_{1/3}Ni_{1/3}O_2$ electrode at a potential of 2.83 V before the first charge/discharge cycle (A) and at a potential of 3.75 V in the third charging process (B).

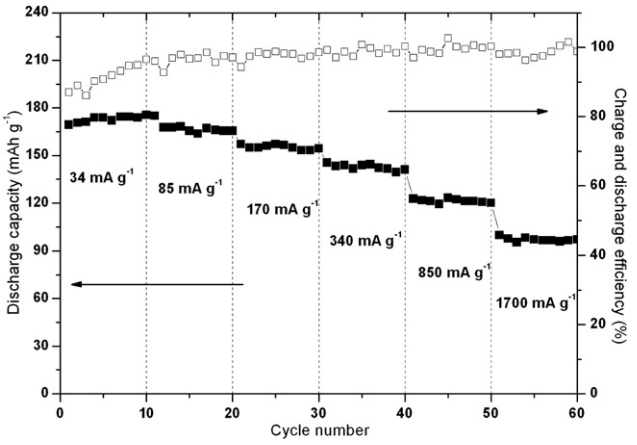


**Fig. 5.** Cycling response of $LiCo_{1/3}Mn_{1/3}Ni_{1/3}O_2$ electrode at various discharge rates and the charge/discharge efficiency.

In order to evaluate the cycling performance of $LiCo_{1/3}Mn_{1/3}Ni_{1/3}O_2$ electrode, the cell was progressively charged and discharged in a series of stages with the charge/discharge rate from 0.2 to 10C. For each stage, the process was taken by 10 cycles. Fig. 5 shows the variation of discharge capacity in this experiment. In the first three cycles at 0.2C, the charge/discharge efficiencies are lower than 90% (87%, 89% and 86%), which means a side reaction possibly related to their large surfaces [3]. Meanwhile, the discharge capacity increased from 170 mAh $g^{-1}$ in the first cycle to 175 mAh $g^{-1}$ in the fourth cycle, which possibly related to the pores in $LiCo_{1/3}Mn_{1/3}Ni_{1/3}O_2$ material. Different pore size, different difficulties to be wetted by electrolyte, so not all of the $LiCo_{1/3}Mn_{1/3}Ni_{1/3}O_2$ particles' surfaces can be wetted by the electrolyte at the same time. As the cycling proceeds, the pores with smaller size may be slowly filtrated by electrolyte, thus more $LiCo_{1/3}Mn_{1/3}Ni_{1/3}O_2$ particles can contact with electrolyte, resulting in a higher discharge capacity. In each stage, the discharge capacity remains very stable even at the rate of 10C. This super cycling performance should be related to the stable structure of $LiCo_{1/3}Mn_{1/3}Ni_{1/3}O_2$ hollow spheres.

## 4. Conclusions

In summary, $LiCo_{1/3}Mn_{1/3}Ni_{1/3}O_2$ hollow spheres prepared by using carbon spheres as template showed an excellent charge/discharge performance. The high capacity even discharge at 10C is mainly due to its nano size of primary particles and large contact surface areas with electrolyte. The excellent cycling performance at different rate is ascribed to its stable hollow structure.

## Acknowledgments

Financial supports from the program of Science Technology Bureau of Shaoxing (2010A21031 and 2012B70017), talent plan of university student of zhejiang province, innovation program of Shaoxing and Natural Science Foundation of China (20901051) are gratefully acknowledged.

## References

[1] T. Ohzuku, Y. Makimura, Chem Lett 30 (2001) 642–643.
[2] S.H. Park, C.S. Yoon, S.G. Kang, H.S. Kim, S.I. Moon, Y.K. Sun, Electrochim Acta 49 (2004) 557–563.
[3] J. Li, C. Daniel, D. Wood, J Power Sources 196 (2011) 2452–2460.
[4] Z. Huang, X. Liu, S. Oh, B. Zhang, P. Ma, J. Kim, J Mater Chem 21 (2011) 10777–10784.
[5] C. Deng, S. Zhang, B.L. Fu, S.Y. Yang, L. Ma, J Alloy Compd 496 (2010) 521–527.
[6] M. Gozu, K. Świerczek, J. Molenda, J Power Sources 194 (2009) 38–44.
[7] J. Liu, W. Qiu, L. Yu, G. Zhang, H. Zhao, T. Li, J Power Sources 174 (2007) 701–704.
[8] F. Wu, M. Wang, Y. Su, L. Bao, S. Chen, J Power Sources 195 (2010) 2900–2904.
[9] S. Zhang, C. Deng, B.L. Fu, S.Y. Yang, L. Ma, Powder Technol 198 (2010) 373–380.
[10] P. Zhang, M. Lin, Q. Yuan, Z. Fan, X. Ren, D. Zhang, Adv Mater Res 92 (2010) 55–64.
[11] K. Du, Z. Peng, G. Hu, Y. Yang, L. Qi, ChemInform 476 (2009) 329–334.
[12] S. Kim, S. Kim, C. Kim, W. Kim, K. Park, Mater Lett 65 (2011) 3313–3316.
[13] X.M. Liu, W.L. Gao, B.M. Ji, J Sol-Gel Sci Technol 61 (2012) 56–61.
[14] K.M. Shaju, P.G. Bruce, Adv Mater 18 (2006) 2330–2334.
[15] Z. Huang, X. Liu, B. Zhang, S. Oh, P. Ma, J. Kim, Scr Mater 64 (2011) 122–125.
[16] Y. Hu, Y. Zhou, J. Wang, Z. Shao, Mater Chem Phys 129 (2011) 296–300.
[17] N.N. Sina, N. Munichandraiah, J Electrochem Soc 157 (2010) A647–A653.
[18] Y. Park, W. Shin, J.W. Lee, Cryst Eng Commun 14 (2012) 4612–4617.
[19] Q. Zhang, Z. Shi, Y. Deng, J. Zheng, G. Liu, G. Chen, J Power Sources 197 (2012) 305–309.
[20] Y. Zhong, X. Wang, K. Jiang, J.Y. Zheng, Y. Guo, Y. Ma, J. Yao, J Mater Chem 21 (2011) 17998–18002.
[21] Y. Deng, Q. Zhang, S. Tang, L. Zhang, S. Deng, Z. Shi, G. Chen, Chem Commun 47 (2011) 6828–6830.
[22] X. Sun, Y. Li, Angew Chem Int Ed 43 (2004) 3827–3831.
[23] M. Zheng, J. Cao, X. Chang, J. Wang, J. Liu, X. Ma, Mater Lett 60 (2006) 2991–2993.
[24] N.D. He, B.S. Wang, J.J. Huang, J. Solid State Electrochem 14 (2010) 1241–1246.
[25] A.M.A. Hashem, A.E. Abdel-Ghany, A.E. Eid, J. Trottier, K. Zaghib, A. Mauger, C.M. Julien, J Power Sources 196 (2011) 8632–8637.
[26] R. Santhanam, B. Rambabu, J Power Sources 195 (2010) 4313–4317.
[27] Z. Yue Wu, J Power Sources 183 (2008) 316–324.
[28] C. Jiang, Y. Zhou, I. Honma, T. Kudo, H. Zhou, J. Power Sources 166 (2007) 514.
[29] D. Li, Y. Kato, K. Kobayakawa, H. Noguchi, Y. Sato, J Power Sources 160 (2006) 1342–1348.